Published in final edited form as:
*JACC Cardiovasc Imaging*. 2011 December ; 4(12): 1284–1293. doi:10.1016/j.jcmg.2011.09.013.

# Multi-Detector Computed Tomography for the Evaluation of Myocardial Cell Therapy in Heart Failure:_A Comparison with Cardiac Magnetic Resonance Imaging

**Karl H. Schuleri, M.D.**[1,*], **Marco Centola, M.D**[1,3], **Seong Hoon Choi, M.D.,Ph.D.**[1,2], **Kristine S. Evers, B.S**[1], **Fady Dawoud, Ph.D.**[1], **Richard T. George, M.D.**[1], **João A.C. Lima, M.D.**[1], and **Albert C. Lardo, Ph.D.**[1,4,*]

[1]The Department of Medicine, Division of Cardiology Johns Hopkins University, Baltimore, MD

[2]The Department of Radiology, Uslan University Hospital, University of Ulsan College of Medicine, Uslan, South Korea

[3]The Division of Cardiology, College of Medicine, Fondazione IRCCS, Azienda Ospedaliera San Paolo, Polo Universitario, Milan, Italy

[4]The Department of Biomedical Engineering Johns Hopkins University, Baltimore, MD

## Abstract

**Objective—**The aim of this study was to use multi-detector computed tomography (MDCT) to assess therapeutic effects of myocardial regenerative cell therapies.

**Background—**Cell transplantation is being widely investigated as a potential therapy in heart failure. Noninvasive imaging techniques are frequently used to investigate therapeutic effects of cell therapies in the preclinical and clinical setting. Previous studies have shown that cardiac MDCT can accurately quantify myocardial scar tissue and determine left ventricular (LV) volumes and ejection fraction (LVEF).

**Methods—**Twenty-two minipigs were randomized to intramyocardial injection of phosphate-buffered saline (placebo, n=9) or 200 million mesenchymal stem cells (MSCs, n=13), twelve weeks after myocardial infarction (MI). Cardiac MRI and MDCT acquisitions were performed prior to randomization 12 weeks after MI induction and at the study endpoint 24 week post-MI. None of the animals received medication to control the intrinsic heart rate during first-pass acquisitions for assessment of LV-volumes and LVEF. Delayed enhancement MDCT imaging was performed 10 min after contrast delivery. Two blinded observers analyzed MDCT acquisitions.

**Results—**MDCT demonstrated that MSC therapy resulted in a reduction of infarct size from 14.3±1.2% to 10.3±1.5% of LV-mass (p=0.005) while infarct size increased in non-treated animals (from 13.8±1.3% to 16.5±1.5%; p=0.02) (Placebo vs MSC; p=0.003). Both observers had excellent agreement for infarct size (r=0.96; p<0.001). LVEF increased from 32.6±2.2% to 36.9±2.7% in MSC treated animals (p=0.03) and decreased in placebo animals (from 33.3±1.4 to 29.1±1.5%; p=0.01; at week 24: placebo vs MSC p=0.02). Infarct size, end-diastolic LV volume



[*]Corresponding Authors **Address for Correspondence:** Albert C. Lardo, Ph.D., F.A.H.A., F.A.C.C and Karl H. Schuleri, M.D. *Image Guided Cardiotherapy Laboratory* Johns Hopkins School of Medicine Division of Cardiology 1042 Ross Building Baltimore, MD 21205 443.287.7490 office 410.502.2067 fax al@jhmi.edu. [*]**Address for Correspondence:** kschuleri@jhmi.edu.

and LVEF assessed by MDCT compared favorably with MRI acquisitions (r=0.70; r=0.82; r=0.902; respectively, p<0.001).

**Conclusions—**This study demonstrates that cardiac MDCT can be used to evaluate infarct size, LV-volumes, and LVEF after intramyocardial delivered MSC therapy. These findings support the use of cardiac MDCT in preclinical and clinical studies for novel myocardial therapies. (word count 299)

### Keywords

MDCT; MRI; Delayed Contrast Enhancement; Göttingen Minipig; Mesenchymal Stem Cell; Myocardial Infarction; Heart failure

## Introduction

Cardiac imaging techniques play a critical role in the evaluation of novel therapies providing reliable surrogate endpoints in the ongoing effort to explore new approaches to treat heart diseases. Myocardial transplantation of different cell types and preparations has been widely investigated as a potential therapy for myocardial infarction (MI) and heart failure (HF) in recent years(1). Magnetic resonance imaging (MRI) is one of the preferred imaging tools in addition to the frequently used echocardiography and nuclear techniques, to provide reliable assessment of left ventricular ejection fractions (LVEF) and infarct size, which are generally accepted surrogate endpoints (2,3). Previous animal studies using cardiac MRI have shown that mesenchymal stem cells (MSC) reduce infarct size and improve LV-function in acute and chronic MI (4–6). However, the use of MRI in the clinical setting is limited in patients with metallic implants and pacemakers, and is relatively complex and time consuming.

Over the last decade, multi-detector computed tomography (MDCT) has emerged as a novel tomographic cardiac imaging modality. Improvement in spatial and temporal resolution has allowed the implementation of myocardial applications, which are necessary to evaluate regenerative therapies. Although, these MDCT applications are still investigative, current MDCT technology is able to provide reliable and reproducible assessment of cardiac function (7,8), myocardial viability with delayed contrast enhancement (de) (9–11), and myocardial blood flow (12–14). However, whether MDCT can be used for follow-up studies and is able to show therapeutic effects of regenerative cell therapies has not been investigated. Accordingly, the purpose of this study was (1) to use MDCT LV-function and myocardial viability as surrogate endpoints in a randomized animal study to evaluate outcomes of intra-myocardial delivered cell therapy and (2) to evaluate the robustness and comparability of MDCT in relation to MRI.

## Methods

### Animal Model

All animal studies were approved by the Johns Hopkins University Institutional Animal Care and Use Committee and comply with the “Guide for the Care and Use of Laboratory Animals” (NIH Publication no. 80–23, revised 1985). Thirty-three female Göttingen minipigs were purchased from Marshall BioResources (North Rose, NY). Myocardial infarcts were induced by occlusion of the mid LAD with an inflated coronary angioplasty balloon as previously described in detail (15). Five animals did not survive the infarct procedure. Two animals died during the early follow-up in the first 4 days post-MI and 4 animals died between week 8 and 12 post-MI. Twenty-two animals were enrolled in the study.

### Cell harvest and isolation

The thirteen animals randomized to cell therapy received bone-marrow derived porcine mesenchymal stem cells (MSCs). MSCs were obtained, isolated, and expanded as previously described (6). In brief, MSC were harvested when they reached 80% to 90% confluence. Cells were then placed in cryo bags at a concentration of 10 to 15 million MSCs / ml and then frozen in a control rate freezer to −180°C until the day of implantation. Trypan blue staining was performed to attest viability of thawed MSC lots before injection. Only MSC lots containing 85% or more of viable cells were used in the study.

### Cell transplantation procedures

Twelve weeks after MI, animals were randomized to receive either intra-myocardial injections of porcine MSCs or phosphate buffered saline (PBS) to serve as a treatment (n=13) or placebo (n=9) group, respectively. Myocardial injections were performed as previously described in detail (5,6).

### Cardiac Multi-Detector Computed Tomography

MDCT images were acquired at two time-points, prior to randomization at week 12 post-MI and 12 weeks after the intra-myocardial injection procedure at week 24.

**Image Acquisition—**Each animal was scanned with electrocardiographic monitoring using a 0.5 mm × 64-slice MDCT scanner (Aquilion™64 -Toshiba Medical Systems Corporation, Otawara, Japan). Data acquisition for LV-function parameters and LV-volumes were initiated manually at a threshold value of 180 HU in the descending aorta. A 60 ml bolus of iodixanol (Visipaque™320 mg iodine/ml; Amersham Health, Amersham, UK) was injected intravenously at rate of 5.0 ml/s opacifiying the LV chamber during first-pass. Additional 90 ml iodixanol were given intravenously after first-pass acquisitions, and delayed contrast enhancement images were acquired 10 minutes after initial contrast delivery; 150-ml of iodixanol (0.91 ± 0.04 × 103 mg iodine/kg body weight) is 1.5 times the human equivalent dose of contrast currently used for MDCT angiography.

During MDCT acquisition, respiration was suspended and imaging was performed using a retrospective ECG-gated MDCT protocol without dose modulation. Imaging parameters: gantry rotation time = 400 ms, detector collimation = 0.5mm × 64 (isotropic voxels = $0.5\times0.5\times0.5$ $mm^3$ - 13 linepairs/cm), helical pitch = variable depending on heart rate (range: 6.4–6.8), tube voltage = 120 kV, tube current = 400 mA). Animals with heart rates >100 beats per minute (bpm) during first-pass acquisition received intravenous metoprolol (2–5 mg) and /or amiodarone (50 to150 mg) to achieve lower heart rate for delayed contrast-enhanced acquisitions.

**Image Reconstruction and Analysis—**All raw data were reconstructed at contiguous 0.5 mm slice thickness by an adaptive multi-segment reconstruction algorithm (16). First-pass acquisitions were reconstructed in 10% steps from 0–90% throughout the entire R–R interval using a standard kernel (FC43); images were reformatted at 4 mm slice thickness in short axis and evaluated in QMass CT® 7.1 (Medis medical imaging systems, Leiden, The Netherlands). Endo- and epicardial borders of the LV were defined in all 10 contiguous slices and each end-diastolic and end-systolic frame was determined to calculate LVEF, end-diastolic LV volume, end-systolic LV volume, LV stroke volume, and LV remodeling parameters. The temporal resolution based on gantry rotation of all MDCT acquisitions was 211.5±5.4 milli-seconds.

Delayed contrast-enhancement MDCT data (for myocardial scar assessment) were reconstructed at 80% of the R to R' interval using the FC43 kernel and multisegment

reconstruction. ECG editing to account for arrhythmias were performed when necessary. Multi-planar reformation at 4 mm slice thickness in the short-axis of the heart was implemented, and MDCT images were analyzed using a custom research software package (Cine Tool, GE Medical Systems Waukesha, WI). Infarct mass/volumes in de-MDCT images were defined by 3 standard deviations (SD) of the signal intensity above the viable myocardium, for the core infarct and 2 SD for the PIZ as described (16). Infarct size was defined as infarct mass as percentage of LV-mass. Both data sets, the cine MDCT acquisitions and de-MDCT images, were analyzed by 2 blinded observers.

### Cardiac Magnetic Resonance Imaging

MRI was performed at the same time-points as MDCT imaging in random order on a 1.5 T MR scanner (CV/i, GE Medical Systems, Waukesha, WI).

**Image Acquisition—**LVEF function and LV volumes were assessed using a steady-state free precession pulse sequence (17). A total of six to eight contiguous short–axis slices were prescribed to cover the entire LV, from base to apex. Image parameters were as follows: TR/TE= 4.2 ms /1.9 ms; flip angle= 45°; 256×160 matrix; 8 mm slice thickness/no gap; 125 kHZ; 28 cm FOV and 1 NSA. After an intravenous injection of Gd-DTPA (0.2 mmol/kg body weight, Magnevist, Berlex, Wayne, NJ), de-MR images were acquired 15 minutes later using an ECG-gated, breath-hold, interleaved, inversion recovery, and FGRE pulse sequence. Delayed contrast enhanced MRI images were acquired in the same location as the short axis cine-images. Imaging parameters were: TR/TE/TI= 7.3 ms, 3.3 ms and 180 to 240 ms; Flip angle= 25°; 256 × 196 matrix; 8 mm slice thickness/no gap; 31.2 kHZ; 28 cm field of view (FOV) and 2 NSA. Inversion recovery time was adjusted as needed to null the normal myocardium (16).

**Image Analysis:** Cine MR images were analyzed with QMass MR® 7.1 (Medis medical imaging systems, Leiden, The Netherlands). To evaluate LVEF, LV-volumes and myocardial mass endo- and epicardial borders were defined each in the end-diastolic and end-systolic frame in 25 to 30 contiguous slices, and LV parameters and volumes were calculated. The temporal resolution of the cine MR images was 21.6±0.9 milliseconds. Delayed contrast enhanced MR images were analyzed on the same custom research software package (Cine Tool, GE Medical Systems, Waukesha, WI) as de-MDCT images. Infarct size, determined by infarct mass as a percentage of LV-mass and infarct volume in de-MR images, were defined with the same threshold method described for de-MDCT analysis.

### Statistical Analysis

All data are presented as mean ± standard error of the mean unless otherwise stated. For infarct size and infarct volume comparison, Pearson correlation and linear regression analysis were used to compare MDCT and MRI. Results were confirmed by Bland-Altman analysis and agreement expressed as mean ±SD difference between methods at 95% confidence intervals (CI). The MDCT and MRI data were evaluated with a paired Student *t*-test. All analyses were performed in MedCalc (MedCalc Software, Mariakerke, Belgium). A $p$-value < 0.05 was considered significant.

## Results

### Baseline conditions

Twenty-two animals were enrolled in this study 12 weeks post-MI (91.9±2.6 days and 87.9±2.0 days post-MI for placebo and MSC, respectively; p=0.19). After randomization, animals in both groups were of similar age (16.8±0.7 months and 15.5±1.1 months for

placebo and MSC, respectively; p=0.35) and body weight (39.3±1.6 kg and 35.7±1.9kg for placebo and MSC, respectively; p=0.11).

### Infarct Size and Scar Volume

One placebo and two MSC treated animals were excluded from analysis due to poor imaging quality caused by motion artifacts at week 24. Infarct size, defined as infarct mass as percentage of LV-mass, was reduced in all MSC treated animals at week 24 while it increased in all animals in the placebo group (Figure 1). We observed a mean expansion of 29.1±5.7% in infarct scar volume in the placebo group ($p$=0.001). MSC therapy had limited effect on total scar volume ($p$=0.1), (Figure 1 and 2 C, D). At week 24, infarct size and infarct volume were reduced in MSC treated animals compared to placebo ($p$=0.003 and $p$=0.01, respectively), (Table 1 and Figure 2 A–D).

### Global LV-Function and LV-Volumes

Cardiac MDCT demonstrated that the decrease in infarct size resulted in 14.0±6.7% improvement in LVEF in animals randomized to MSC therapy, whereas LVEF decreased by - 12.3±3.1% in the placebo group (Table 1 and Figure 2E, F). Of note, 2 animals that received MSC therapy did not show improved LVEF (Figure 2F). All MDCT data for global LV-function and LV-volumes are summarized in table 1.

### Inter-Observer Variability

Inter-observer correlation for infarct size, total infarct volume, LVEF, and end-diastolic LV-volumes were excellent (r=0.96, r=0.98, r=0.93 and r=0.93, respectively) in MDCT acquisitions. The complete data is presented in table 2.

### MDCT comparison with MRI

MDCT and MRI were performed on the same day in random order within two hours following the first imaging study. Three animals had to be excluded from the analysis as MRI data were not obtained on the day of the MDCT imaging. In 32 MRI studies, available the same day as MDCT acquisitions, we found fair agreement for infarct size, infarct volume, LVEF, and end-diastolic LV volume (Figure 3 and table 3). In addition, end-systolic LV volumes showed a good correlation with both imaging modalities (r=0.81; p<0.001). Bland-Altman analysis revealed a slight overestimation by 1.4 mL (CI: 16.3 to −13.6) with MDCT. Table 4 shows a direct comparison of all MDCT and MRI values at the two time-points.

Finally, we showed that MDCT and MRI demonstrate similar effectiveness of MSC therapy from week 12 to week 24 (Figure 4). Infarct size decreased by mean values of 4.7±1.1 cc and 6.2±2.0 cc when evaluated with de-MDCT and de-MRI in MSC treated animals, respectively ($p$=0.43). The changes in LVEF with MSC treatment were also apparent with both imaging modalities with comparable mean values (4.5±1.0 mL and 5.6±1.3 mL, MDCT vs. MRI, respectively; $p$=0.4). The changes between the in placebo and MSC treated animals were also detected with both imaging modalities. Although the detected differences between MDCT and MRI were not significant for all infarct and functional parameters, the changes over time (Δchange) correlated assessment (Figure4).

## Discussion

This is the first study to employ cardiac MDCT for the evaluation of therapeutic effects of cell therapy on infarct size, LV-volumes, and LV-function. Our results suggest that MDCT imaging reliably assesses end-diastolic LV volumes, LVEF, infarct size, and infarct volumes with delayed contrast acquisitions; it is able to access the effect of intra-myocardial

delivered cell therapy compared to placebo. These findings confirm previous studies that used MRI to evaluate the therapeutic potential of intra-myocardial delivered MSC in HF subjects with chronic infarct scars (6,18). This study introduces MDCT imaging as an alternative cardiac imaging technique to determine efficacy of novel myocardial therapeutics.

## Myocardial Infarct Scar Assessment by MDCT

MDCT has the capability to distinguish between viable and non-viable myocardium with delayed contrast-enhancement for the detection of acute and chronic infarct scar, and has recently been reported in animal experiments and human studies; however, it is still considered an investigative technique (9–11,16,19). After intravenous delivery, iodine-based contrast agents accumulate in myocardial tissue damaged by MI. The discrimination between viable and nonviable myocardium result from increased attenuation values caused by the accumulation of iodine molecules in the infarct area detected by MDCT. This is in contrast to enhancement mechanisms by MRI that rely on alteration of the contrast media via interactions with water molecules (9). The infarct sizes detected by de-MDCT in this study are significantly smaller than matching MRI values; these results are in accordance with previously published data for acute and chronic MI (16,20). Thus, de-MDCT and de-MRI derived values for infarct size and infarct volume should not be used interchangeable at the current status of MDCT technology.

The extent of contrast enhancement detected by MRI has been shown to predict the response to medical treatment in HF patients (21). Reduction of infarct size has been noted with de-MRI following myocardial cell therapy in animal studies and patients (4–6,22,23). Thus, quantification of infarct size and infarct volume by de-MDCT could be a valuable surrogate end point allowing the prediction of response to therapy. Delayed contrast enhanced MDCT currently offers the highest spatial resolution for transmural characterization of infarct scars, and this can be particularly helpful in guiding intra-myocardial delivery of cell-based therapies. An akinetic segment might be deemed nonviable by nuclear techniques caused by limited spatial resolution, but shows some viability in de-MDCT, which increases the likelihood that this segment will eventually recover with therapeutic intervention (24).

## Evaluation of Cardiac Function and Volumes by MDCT

Cardiac function with MDCT is accomplished with intravenous injection of iodine-based contrast agents for opacification of the blood pool to delineate the borders of the ventricle and application of retrospective ECG-gated protocols, to record the complete cardiac cycle during the R-R-interval. Various investigators reported a consistent overestimation of LVES volumes and an underestimation of LVEF by MDCT with 4-slice and early 16-slice technology compared to MRI; however, with the introduction of 64-slice MDCT technology and improvement in temporal resolution these inter-method differences in global LV function variables are no longer reproduced. Temporal resolution, based on gantry rotation, has been reported to be less than 165 ms with single-source systems and further to 83ms with dual-source MDCT technology (7). Our results are in accordance with studies comparing single-source and dual-source 64-slice MDCT— with MRI showing small differences between both modalities and narrow Bland-Altman windows (25–29). In our study, we observed good correlation coefficients for end-diastolic LV-volumes and LVEF and we are able to confirm the linear relationship between both volumetric imaging techniques for LV-function and LV remodeling parameters making both tomographic imaging methods interchangeable for LV function and LV-volumes assessment. Evaluation of the cardiac structure, LV-volumes, and LV-function—specifically LVEF— is an integral step in determining prognosis and therapy for HF patients (30). Human trials, using a variety of cell-therapy approaches, have used improvements in LVEF as an end-point (3).

Compared with volumetric changes, using LVEF as an end-point has the advantage of denoting a survival difference and is an accepted surrogate measure for mortality (31). The magnitude of treatment effect on LVEF seen in these trials has ranged from 5% to 9%, while the change in the control groups has ranged from −2% to 4% (32).

## Advantages and Limitation of MDCT imaging

As a novel cardiac imaging option for LV-function and viability, MDCT offers some solutions for the difficulties faced in MRI. MDCT can be safely performed in patients with metallic implants, such as pacemakers; defibrillators; and prostheses; who are inappropriate candidates for MRI. Although MRI is considered the reference standard for cardiac function and myocardial viability— based on the accuracy and reproducibility of measurements— the duration of cardiac MRI acquisitions with multiple prolonged breath-holds are required to obtain adequate data sets, are time consuming, and impossible in patients with claustrophobia. Thus, cardiac MRI is limited to specialized centers, which is in contrast to cardiac MDCT which is widely accessible. MDCT imaging is fast and offers good temporal and excellent spatial resolution; however, MDCT acquisitions require iodinated contrast agents and involve radiation exposure.

## Future Perspective

In order to translate cardiac function and viability assessment with MDCT into clinical trials standardized low-dose protocols are needed; especially, to minimize overall radiation exposure as follow–up studies are required for outcome assessment. In the latest generation of MDCT scanners, ECG-gated tube current modulations are commonly applied in retrospective acquisitions for evaluation of cardiac function (7). Low-dose delayed contrast-enhancement protocols have been reported (9). We have recently described a prospectively gated protocol for high-resolution de-MDCT imaging that lowers radiation dose by an order of magnitude (33).

In addition to cardiac function and viability, MDCT is able to assess myocardial blood flow (MBF). Cardiac CT perfusion is based on the same first-pass principle as MRI (14) which has been used to evaluate cell therapy (5). Semi-quantitative and quantitative assessments of MBF with MDCT have been reported in experimental animals (9,13). Cardiac MDCT is poised to offer a comprehensive evaluation of novel myocardial therapeutics.

## Study Limitations

This animal study was conducted without any medical therapy given to patients currently post-MI. Therefore, the chronic MIs expanded and the infarct size increased in the placebo group consistent with results from a clinical study using non-invasive imaging techniques conducted in the early 1980s (34). With modern medical therapy decrease in infarct size is anticipated in chronic MI as shown in a recent MRI study (35). To complicate matters, additive effects of ACE inhibition with β-blockade in combination with cell therapy are described (36). Although these limitations are evident in the current study, the goal of this study was to demonstrate the usefulness of using MDCT to evaluate the effect of myocardial therapies.

However, there are some limitations that may affect the transfer of the reported MDCT protocols and results to application in human trials. First, the animals presented had elevated heart rates which are usually considered a relative contraindication for MDCT. While the reported MDCT protocols proved reliable even under these unfavorable conditions, it has to be considered that patients with an elevated heart rate above 60–70bpm may receive negative chronotropic medication in order to reduce the heart rate for coronary CT angiography. This will affect the value of functional analysis, as ventricular volumes change

if beta blockers are applied; however, beta blockers only have to be given if coronary CT angiography is mandated. Second, no tube current modulation was applied, as is routinely done now in patient studies in order to reduce radiation exposure. Increased image noise on systolic images of ECG-gated tube current modulation may affect the accuracy of global and regional LV function assessment. Third, because of the passive contrast kinetics of iodine-based contrast agents and the limited collateral circulation in pigs, de-MDCT imaging of chronic infarct scars in this animal model requires a relatively large dose of iodine to cause a sufficient change in the volume distribution in the myocardial bed. In this study we used 1.5 times a human equivalent dose, though successful viability imaging in humans has been reported in several studies with standard contrast volumes used for coronary CT angiography (37).

### Conclusions

This animal study suggests that cardiac MDCT can be reliably used to evaluate infarct size, infarct volumes, LV-volumes, and LV–function after intra-myocardial delivered MSC therapy with sensitivity similar to cardiac MRI showing similar changes at follow-up. These findings support the use of cardiac MDCT in preclinical and clinical studies as a non-invasive imaging technique for detecting therapeutic effects of novel myocardial therapies.

## Abbreviation List

| | |
|---|---|
| **de** | delayed contrast-enhancement |
| **LAD** | left anterior descending artery |
| **LV** | left ventricle/ventricular |
| **LVEDV** | left ventricular end-diastolic volume |
| **LVESV** | left ventricular end-systolic volume |
| **LVEF** | left ventricular ejection fraction |
| **LVSV** | left ventricular systolic volume |
| **MDCT** | multi-detector computed tomography |
| **MI** | myocardial infarction |
| **MSC** | mesenchymal stem cell |
| **MRI** | magnetic resonance imaging |
| **SD** | standard deviation |

## References

1. Wollert KC, Drexler H. Cell therapy for the treatment of coronary heart disease: a critical appraisal. Nat Rev Cardiol. 7:204–15. [PubMed: 20177405]
2. Lau JF, Anderson SA, Adler E, Frank JA. Imaging approaches for the study of cell-based cardiac therapies. Nat Rev Cardiol. 7:97–105. [PubMed: 20027188]
3. Beeres SL, Bengel FM, Bartunek J, et al. Role of imaging in cardiac stem cell therapy. J Am Coll Cardiol. 2007; 49:1137–48. [PubMed: 17367656]
4. Amado LC, Saliaris AP, Schuleri KH, et al. Cardiac repair with intramyocardial injection of allogeneic mesenchymal stem cells after myocardial infarction. Proc Natl Acad Sci U S A. 2005; 102:11474–9. [PubMed: 16061805]
5. Schuleri KH, Amado LC, Boyle AJ, et al. Early improvement in cardiac tissue perfusion due to mesenchymal stem cells. Am J Physiol Heart Circ Physiol. 2008; 294:H2002–11. [PubMed: 18310523]

6. Schuleri KH, Feigenbaum GS, Centola M, et al. Autologous mesenchymal stem cells produce reverse remodelling in chronic ischaemic cardiomyopathy. Eur Heart J. 2009; 30:2722–32. [PubMed: 19586959]
7. Sayyed SH, Cassidy MM, Hadi MA. Use of multidetector computed tomography for evaluation of global and regional left ventricular function. J Cardiovasc Comput Tomogr. 2009; 3:S23–34. [PubMed: 19138579]
8. Savino G, Zwerner P, Herzog C, et al. CT of cardiac function. J Thorac Imaging. 2007; 22:86–100. [PubMed: 17325580]
9. Schuleri KH, George RT, Lardo AC. Applications of cardiac multidetector CT beyond coronary angiography. Nat Rev Cardiol. 2009; 6:699–710. [PubMed: 19851349]
10. Gerber BL, Belge B, Legros GJ, et al. Characterization of acute and chronic myocardial infarcts by multidetector computed tomography: comparison with contrast-enhanced magnetic resonance. Circulation. 2006; 113:823–33. [PubMed: 16461822]
11. Lardo AC, Cordeiro MA, Silva C, et al. Contrast-enhanced multidetector computed tomography viability imaging after myocardial infarction: characterization of myocyte death, microvascular obstruction, and chronic scar. Circulation. 2006; 113:394–404. [PubMed: 16432071]
12. George RT, Arbab-Zadeh A, Miller JM, et al. Adenosine stress 64- and 256-row detector computed tomography angiography and perfusion imaging: a pilot study evaluating the transmural extent of perfusion abnormalities to predict atherosclerosis causing myocardial ischemia. Circ Cardiovasc Imaging. 2009; 2:174–82. [PubMed: 19808590]
13. George RT, Jerosch-Herold M, Silva C, et al. Quantification of myocardial perfusion using dynamic 64-detector computed tomography. Invest Radiol. 2007; 42:815–22. [PubMed: 18007153]
14. Schuleri KH, George RT, Lardo AC. Assessment of coronary blood flow with computed tomography and magnetic resonance imaging. J Nucl Cardiol. 17:582–90. [PubMed: 20585916]
15. Schuleri KH, Boyle AJ, Centola M, et al. The adult Gottingen minipig as a model for chronic heart failure after myocardial infarction: focus on cardiovascular imaging and regenerative therapies. Comp Med. 2008; 58:568–79. [PubMed: 19149414]
16. Schuleri KH, Centola M, George RT, et al. Characterization of peri-infarct zone heterogeneity by contrast-enhanced multidetector computed tomography: a comparison with magnetic resonance imaging. J Am Coll Cardiol. 2009; 53:1699–707. [PubMed: 19406346]
17. Slavin GS, Saranathan M. FIESTA-ET: high-resolution cardiac imaging using echo-planar steady-state free precession. Magn Reson Med. 2002; 48:934–41. [PubMed: 12465101]
18. Quevedo HC, Hatzistergos KE, Oskouei BN, et al. Allogeneic mesenchymal stem cells restore cardiac function in chronic ischemic cardiomyopathy via trilineage differentiating capacity. Proc Natl Acad Sci U S A. 2009; 106:14022–7. [PubMed: 19666564]
19. le Polain de Waroux JB, Pouleur AC, Goffinet C, Pasquet A, Vanoverschelde JL, Gerber BL. Combined coronary and late-enhanced multidetector-computed tomography for delineation of the etiology of left ventricular dysfunction: comparison with coronary angiography and contrast-enhanced cardiac magnetic resonance imaging. Eur Heart J. 2008; 29:2544–51. [PubMed: 18762553]
20. Baks T, Cademartiri F, Moelker AD, et al. Multislice computed tomography and magnetic resonance imaging for the assessment of reperfused acute myocardial infarction. J Am Coll Cardiol. 2006; 48:144–52. [PubMed: 16814660]
21. Bello D, Shah DJ, Farah GM, et al. Gadolinium cardiovascular magnetic resonance predicts reversible myocardial dysfunction and remodeling in patients with heart failure undergoing beta-blocker therapy. Circulation. 2003; 108:1945–53. [PubMed: 14557364]
22. Britten MB, Abolmaali ND, Assmus B, et al. Infarct remodeling after intracoronary progenitor cell treatment in patients with acute myocardial infarction (TOPCARE-AMI): mechanistic insights from serial contrast-enhanced magnetic resonance imaging. Circulation. 2003; 108:2212–8. [PubMed: 14557356]
23. Dill T, Schachinger V, Rolf A, et al. Intracoronary administration of bone marrow-derived progenitor cells improves left ventricular function in patients at risk for adverse remodeling after acute ST-segment elevation myocardial infarction: results of the Reinfusion of Enriched

Progenitor cells And Infarct Remodeling in Acute Myocardial Infarction study (REPAIR-AMI) cardiac magnetic resonance imaging substudy. Am Heart J. 2009; 157:541–7. [PubMed: 19249426]

24. Kim RJ, Shah DJ. Fundamental concepts in myocardial viability assessment revisited: when knowing how much is “alive” is not enough. Heart. 2004; 90:137–40. [PubMed: 14729777]
25. Annuar BR, Liew CK, Chin SP, et al. Assessment of global and regional left ventricular function using 64-slice multislice computed tomography and 2D echocardiography: a comparison with cardiac magnetic resonance. Eur J Radiol. 2008; 65:112–9. [PubMed: 17466480]
26. Bruners P, Mahnken AH, Knackstedt C, et al. Assessment of global left and right ventricular function using dual-source computed tomography (DSCT) in comparison to MRI: an experimental study in a porcine model. Invest Radiol. 2007; 42:756–64. [PubMed: 18030198]
27. Busch S, Johnson TR, Wintersperger BJ, et al. Quantitative assessment of left ventricular function with dual-source CT in comparison to cardiac magnetic resonance imaging: initial findings. Eur Radiol. 2008; 18:570–5. [PubMed: 17909817]
28. Palumbo A, Maffei E, Martini C, et al. Functional parameters of the left ventricle: comparison of cardiac MRI and cardiac CT in a large population. Radiol Med. 115:702–13. [PubMed: 20177984]
29. Mahnken AH, Bruners P, Bornikoel CM, et al. Dual-source CT assessment of ventricular function in healthy and infarcted myocardium: An animal study. Eur J Radiol. 2009
30. Hunt SA, Abraham WT, Chin MH, et al. 2009 focused update incorporated into the ACC/AHA 2005 Guidelines for the Diagnosis and Management of Heart Failure in Adults: a report of the American College of Cardiology Foundation/American Heart Association Task Force on Practice Guidelines: developed in collaboration with the International Society for Heart and Lung Transplantation. Circulation. 2009; 119:e391–479. [PubMed: 19324966]
31. Rector TS, Cohn JN. Prognosis in congestive heart failure. Annu Rev Med. 1994; 45:341–50. [PubMed: 8198388]
32. Fuster V, Sanz J, Vile-Gonzalez JF, Rajagopalan S. The utility of magnetic resonance imaging in cardiac tissue regeneration trials. Nat Clin Pract Cardiovasc Med. 2006; 3(Suppl 1):S2–7. [PubMed: 16501625]
33. Chang HJ, George RT, Schuleri KH, et al. Prospective electrocardiogram-gated delayed enhanced multidetector computed tomography accurately quantifies infarct size and reduces radiation exposure. JACC Cardiovasc Imaging. 2009; 2:412–20. [PubMed: 19580722]
34. Erlebacher JA, Weiss JL, Eaton LW, Kallman C, Weisfeldt ML, Bulkley BH. Late effects of acute infarct dilation on heart size: a two dimensional echocardiographic study. Am J Cardiol. 1982; 49:1120–6. [PubMed: 6461240]
35. Engblom H, Hedstrom E, Heiberg E, Wagner GS, Pahlm O, Arheden H. Rapid initial reduction of hyperenhanced myocardium after reperfused first myocardial infarction suggests recovery of the peri-infarction zone: one-year follow-up by MRI. Circ Cardiovasc Imaging. 2009; 2:47–55. [PubMed: 19808564]
36. Boyle AJ, Schuster M, Witkowski P, et al. Additive effects of endothelial progenitor cells combined with ACE inhibition and beta-blockade on left ventricular function following acute myocardial infarction. J Renin Angiotensin Aldosterone Syst. 2005; 6:33–7. [PubMed: 16088849]
37. Nieman K, Shapiro MD, Ferencik M, et al. Reperfused myocardial infarction: contrast-enhanced 64-Section CT in comparison to MR imaging. Radiology. 2008; 247:49–56. [PubMed: 18372464]

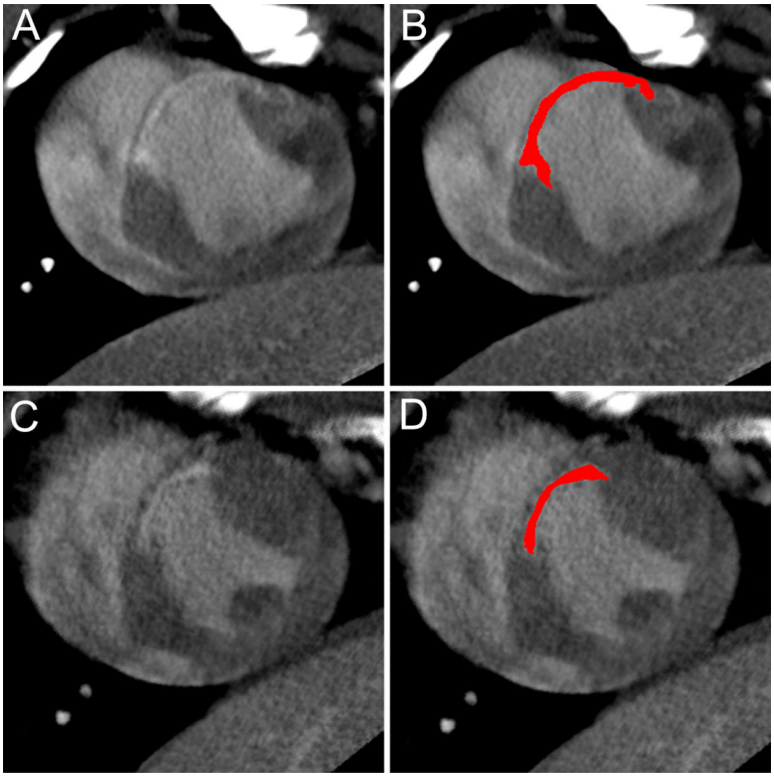


**Figure 1. Infarct assessment with delayed contrast enhanced MDCT**

Example of de-MDCT images for a placebo (A,B) and a MSC (C,D) treated animal at 24 weeks. Delayed contrast enhanced images were reconstructed in the short axis at 4 mm slice thickness. Panel B and D show the slices of the placebo (A) and MSC (C) case, respectively, with a computer-generated mask depicting the infarct area in red.

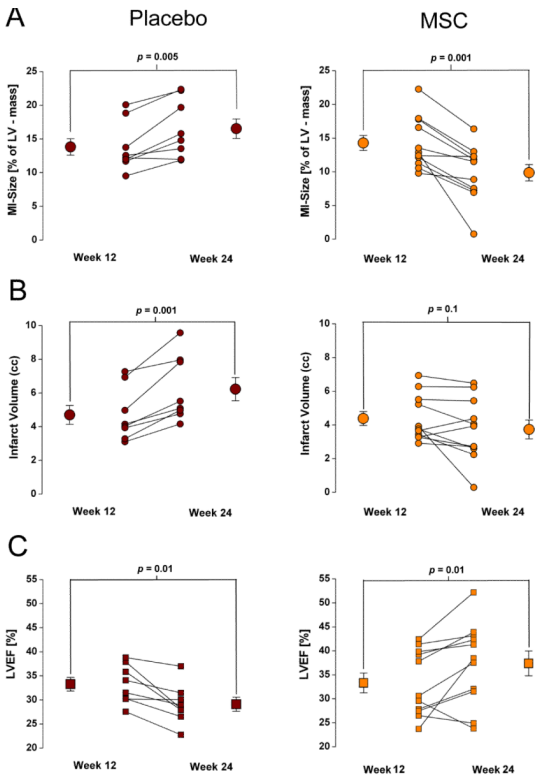


**Figure 2. Impact of MSC Therapy assessed by MDCT**

(A–D) All placebo animals (n=8) showed an increase in infarct size (A) and infarct volume (C) at week 24, while intra-myocardial delivery of MSCs reduced infarct size (B) and stabilized infarct volume (D) in all treated animals (n=11).(E, F) LVEF is decreased at week 24 in placebo animals, while it increases in most MSC treated animals; however, in 2 animals the treatment failed to improve LVEF.

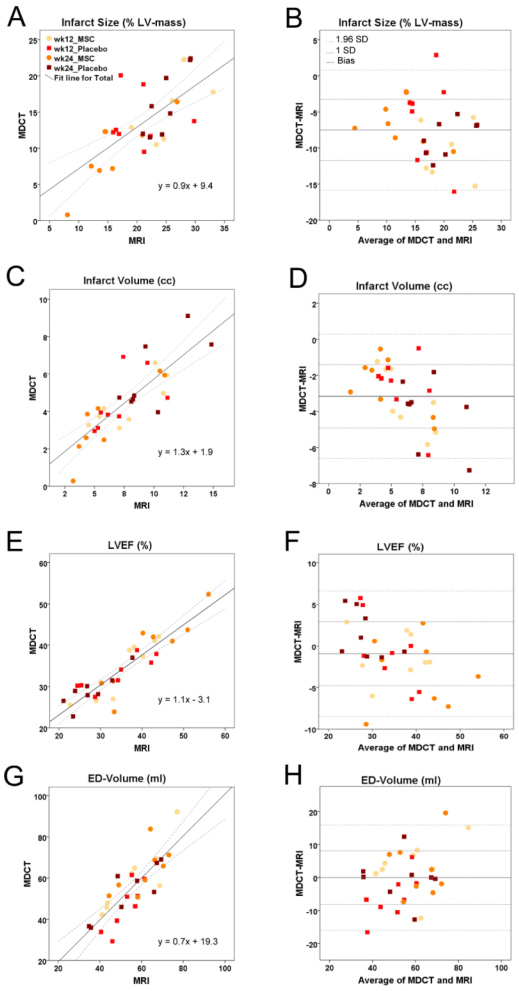


**Figure 3. Quantitative Assessment of MDCT and MRI values**

The relation between MDCT and MRI for infarct size, infarct volume, LVEF and LVED-volume was evaluated for 16 animals at both time-points. (A, B) MDCT and MRI show a fair correlation for infarct size at 4 mm and 8 mm slice thickness, respectively, with an underestimation of infarct size by de- MDCT compared to de-MRI in Bland-Altman analysis. (C, D) Good correlation of infarct volume with less underestimation of by de-MDCT than infarct size. (E, F) Good correlation of both modalities can be appreciated with minimal underestimation of LVEF by MDCT. (G,H) MDCT and MRI show excellent correlation of end-diastolic volume.

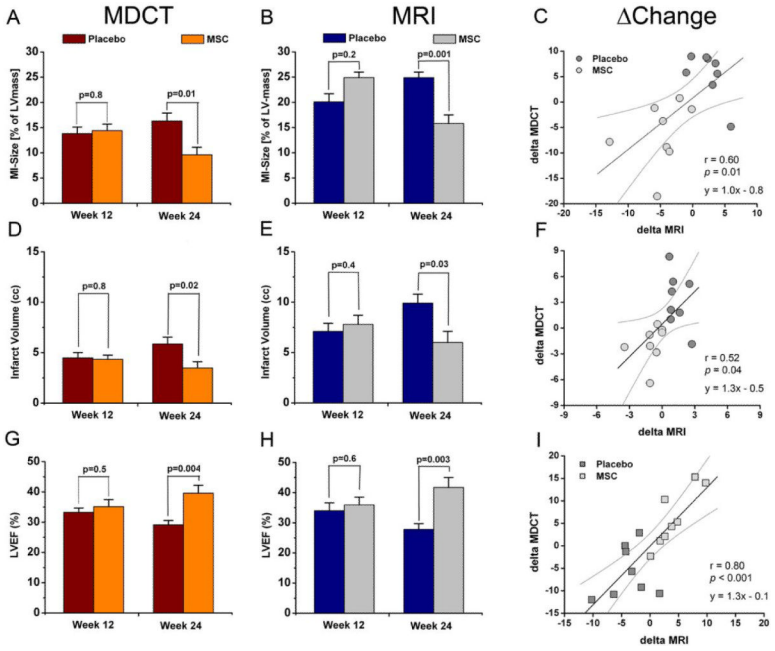


**Figure 4. Comparison of MDCT and MRI values for MI and LVEF assessment**

Data of placebo (n=8) and MSC treated (n=8) animals imaged on the same day with both modalities are compared to evaluate the absolute difference of MDCT and MRI values, effectiveness of MSC therapy and correlation of the evaluated changes over time (Δchange). (A,B) Both de-MDCT and de-MRI detect significant differences of infarct size with MSC therapy ($p<0.0001$). (C) The changes over time show a fair correlation between MDCT and MRI assessment. (D,E,F) These differences are also apparent as infarct volume is compared ($p<0.0001$) showing a modest correlation of both modalities. (G,H) Values for LVEF are similar with MDCT and MRI. Importantly, the effectiveness of MSC therapy is apparent with both imaging modalities, and detected changes were not significantly different between MDCT and MRI evaluations in the studied animals ($p=0.06$). (I) The Δchange analysis shows a good correlation for LVEF evaluation with MDCT and MRI.

**Table 1**

Infarct values, LV-Function and LV-Volumes by MDCT

| Parameter | | Groups | Week 12 | Week 24 | *p*-value |
|---|---|---|---|---|---|
| **Infarct size** | (% of LVmass) | Placebo | 13.8 ± 1.3 | 16.3 ± 1.6 | *0.005* |
| | | MSC | 14.3 ± 1.2 | 9.9 ± 1.3$^{*}$ | *0.001* |
| **Total infarct volume** | (cc) | Placebo | 4.7 ± 0.6 | 6.2 ± 0.7 | *0.001* |
| | | MSC | 4.4 ± 0.4 | 3.6 ± 0.5$^{\dagger}$ | *0.1* |
| **LVED mass** | (g) | Placebo | 33.6 ± 1.1 | 37.5 ± 1.6 | *0.02* |
| | | MSC | 30.6 ± 1.3 | 37.4 ± 2.1$^{\#}$ | *0.0003* |
| **LV ejection fraction** | (%) | Placebo | 33.3 ± 1.4 | 29.1 ± 1.5 | *0.01* |
| | | MSC | 32.6 ± 2.2 | 36.9 ± 2.7$^{\S}$ | *0.03* |
| **Stroke volume** | (ml) | Placebo | 19.7 ± 1.6 | 19.4 ± 0.8 | *0.81* |
| | | MSC | 15.1 ± 0.7 | 20.6 ± 1.6$^{\#}$ | *0.004* |
| **LVED volume** | (ml) | Placebo | 60.1 ± 5.7 | 67.6 ± 4.1 | *0.16* |
| | | MSC | 48.1 ± 3.1 | 56.3 ± 4.3$^{\#}$ | *0.01* |
| **LVES volume** | (ml) | Placebo | 40.4 ± 4.5 | 48.3 ± 3.7 | *0.07* |
| | | MSC | 33.0 ± 2.9 | 36.4 ± 4.1$^{**}$ | *0.15* |

MSC (n=11) vs Placebo (n=8)

$^{*}$ *p*=0.003

$^{\#}$ *p*=NS

$^{**}$ *p*=0.047

$^{\dagger}$ *p*=0.01

$^{\S}$ *p*=0.02

$^{\#}$ p=NS

**Table 2**

Inter-Observer Variability for MDCT

| Parameters | | Correlation Coefficient (r) | 95% Confidence Interval for r | Significance Level *(p)* | Difference (mean) | 95% Confidence interval for mean |
|---|---|---|---|---|---|---|
| **Infarct size** | (% of LVmass) | 0.96 | 0.93 to 0.98 | *<0.0001* | 0.6 | 3.0 to −1.8 |
| **Infarct volume** | (ml) | 0.98 | 0.95 to 0.99 | *<0.0001* | 0.05 | 0.8 to −0.7 |
| **LVED mass** | (gram) | 0.84 | 0.71 to 0.92 | *<0.0001* | −0.9 | 3.9 to −5.7 |
| **LV ejection fraction** | (%) | 0.93 | 0.87 to 0.96 | *<0.0001* | −1.1 | 4.8 to −7.0 |
| **Stroke volume** | (ml) | 0.84 | 0.70 to 0.91 | *<0.0001* | −0.1 | 5.2 to −5.3 |
| **ED volume** | (ml) | 0.92 | 0.84 to 0.96 | *<0.0001* | 3.1 | 14.9 to −8.7 |
| **ES volume** | (ml) | 0.93 | 0.86 to 0.96 | *<0.0001* | 3.2 | 12.7 to −6.2 |

**Table 3**

Correlation and Bland-Altman Analysis of MDCT and MRI

| Parameters | | | Correlation Coefficient (r) | Linear Regression Equation | Signifficance Level (*p*) | mean Difference (bias) | Standard Deviation (SD) | 95% Confidence interval for mean |
|---|---|---|---|---|---|---|---|---|
| **Infarct size** | (% L Vmass) | Total | 0.70 | y = 0.9 x + 9.4 | *<0.0001* | −7.5 | 4.27 | 0.8 to −15.9 |
| | | week 12 | 0.37 | y = 0.5 x + 14.1 | *0.16* | −7.5 | 5.23 | 3.0 to −18.0 |
| | | week 24 | 0.89 | y = 1.0 x + 7.5 | *<0.0001* | −7.5 | 3.06 | −1.7 to −13.3 |
| | | placebo | 0.44 | y = 0.5 x + 15.4 | *0.09* | −7.4 | 4.22 | 1.7 to −16.5 |
| | | MSC | 0.82 | y = 1.1 x + 6.1 | *<0.001* | −7.6 | 4.07 | 0.2 to −15.4 |
| **Total infarct volume** | (cc) | Total | 0.81 | y = 1.3 x + 1.9 | *<0.0001* | −3.2 | 1.71 | 0.3 to −6.6 |
| | | week 12 | 0.68 | y = 1.2 x + 2.3 | *0.004* | −3.0 | 1.77 | 0.3 to −6.4 |
| | | week 24 | 0.87 | y = 1.3 x + 1.9 | *<0.0001* | −3.3 | 1.76 | 0.3 to −6.9 |
| | | placebo | 0.73 | y = 1.1 x + 2.7 | *0.001* | −3.3 | 1.94 | 0.4 to −7.0 |
| | | MSC | 0.86 | y = 1.5 x + 1.2 | *<0.0001* | −3.0 | 1.53 | 0.3 to −6.2 |
| **LV ejection fraction** | (%) | Total | 0.90 | y = 1.1 x − 3.2 | *<0.0001* | −0.9 | 3.81 | 6.6 to −8.5 |
| | | week 12 | 0.87 | y = 1.1 x − 2.4 | *<0.0001* | −0.9 | 3.69 | 6.1 to −8.0 |
| | | week 24 | 0.92 | y = 1.1 x − 3.5 | *<0.0001* | −0.9 | 4.19 | 7.3 to −9.1 |
| | | placebo | 0.88 | y = 1.4 x − 12.1 | *<0.0001* | 0.3 | 3.43 | 7.6 to −7.0 |
| | | MSC | 0.91 | y = 1.0 x − 3.6 | *<0.0001* | −2.2 | 3.78 | 5.0 to −9.6 |
| **ED volume** | (ml) | Total | 0.82 | y = 0.7 x + 19.3 | *<0.0001* | −0.02 | 6.63 | 15.9 to −16.0 |
| | | week 2 | 0.84 | y = 0.6 x + 23.6 | *<0.001* | −1.2 | 5.90 | 15.7 to −18.0 |
| | | week 24 | 0.81 | y = 0.8 x + 12.2 | *<0.001* | 1.1 | 7.44 | 16.3 to −14.1 |
| | | placebo | 0.81 | y = 0.7 x + 18.5 | *<0.001* | −3.1 | 6.38 | 11.1 to −17.3 |
| | | MSC | 0.81 | y = 0.7 x + 15.9 | *<0.001* | 3.0 | 7.10 | 18.8 to −12.7 |

Total: n=32; week 12, week 24, placebo, MSC: n=16

**Table 4**

Comparison of MDCT and MRI studies (n=32)

| Parameter | | Groups | Placebo | | *p*-value | MSC | | *p*-value |
|---|---|---|---|---|---|---|---|---|
| | | | week 12 | week 24 | | week 12 | week 24 | |
| Infarct Size | (% of LV mass) | MDCT | 13.8 ± 1.3 | 16.3 ± 1.6 | *0.02* | 14.5 ± 1.4 | 9.4 ± 1.7* | *0.005* |
| | | MRI | 20.1 ± 1.6 | 24.9 ± 1.1 | *0.03* | 23.3 ± 2.1 | 15.8 ± 2.0† | *0.01* |
| Total infarct volume | (cc) | MDCT | 4.5 ± 0.5 | 5.9 ± 0.7 | *0.002* | 4.4 ± 0.5 | 3.5 ± 0.7§ | *0.04* |
| | | MRI | 7.1 ± 0.8 | 9.9 ± 0.9 | *0.03* | 7.8 ± 0.9 | 6.0 ± 1.1 | *0.04* |
| LVED mass | (g) | MDCT | 35.0 ± 1.4 | 37.8 ± 1.4 | *0.08* | 33.5 ± 1.6 | 39.4 ± 2.8 | *0.10* |
| | | MRI | 37.3 ± 2.5 | 41.3 ± 2.4 | *0.16* | 32.2 ± 1.9 | 37.8 ± 1.4 | *0.05* |
| LV ejection fraction | (%) | MDCT | 33.3 ± 1.4 | 29.1 ± 1.5 | *0.03* | 34.7 ± 2.5 | 38.5 ± 3.2# | *0.02* |
| | | MRI | 34.0 ± 2.6 | 27.8 ± 1.9 | *0.01* | 35.9 ± 2.6 | 41.7 ± 3.3†† | *0.02* |
| ED volume | (ml) | MDCT | 60.1 ± 5.7 | 67.6 ± 4.1 | *0.16* | 48.7 ± 4.0 | 54.7 ± 3.8** | *0.44* |
| | | MRI | 56.6 ± 4.7 | 65.1 ± 2.5 | *0.08* | 50.2 ± 3.5 | 53.5 ± 4.69** | *0.67* |

week 24: MSC (n=8) vs Placebo (n=8);

* *p*=0.01

† *p*=0.001

§ *p*=0.03

# p=0.02

** *p*=0.04

†† *p*=0.003